EFDA–JET–PR(07)18

X. Litaudon, G. Arnoux, M. Beurskens, S. Brezinsek, C.D. Challis, F. Crisanti, P.C. De Vries, C. Giroud, R.A. Pitts, F.G. Rimini, Y. Andrew, M. Ariola, Yu F. Baranov, M. Brix, P. Buratti, R. Cesario, Y. Corre, E. De La Luna, W. Fundamenski, E. Giovannozzi, M.P. Gryaznevich, N.C. Hawkes, J. Hobirk, A. Huber, S. Jachmich, E. Joffrin, H.R. Koslowski, Y. Liang, Th. Loarer, P. Lomas, T. Luce, J. Mailloux, G.F. Matthews, K. McCormick, D. Mazon, D. Moreau, V. Pericoli, V. Philipps, E. Rachlew, S.D.A Reyes-Cortes, G. Saibene, S.E. Sharapov, I. Voitsekovitch, L Zabeo, O. Zimmermann, K.D. Zastrow and the JET-EFDA contributors*

# Development of Steady-State Scenarios Compatible with ITER-like Wall Conditions

# Development of Steady-State Scenarios Compatible with ITER-like Wall Conditions

X. Litaudon[1], G. Arnoux[1], M. Beurskens[2], S. Brezinsek[3], C.D. Challis[2], F. Crisanti[4], P.C. De Vries[2], C. Giroud[2], R.A Pitts[5], F.G. Rimini[1], Y. Andrew[2], M. Ariola[4], Yu F. Baranov[2], M. Brix[2], P. Buratti[4], R. Cesario[4], Y. Corre[1], E. De La Luna[6], W. Fundamenski[2], E. Giovannozzi[4], M.P. Gryaznevich[2], N.C. Hawkes[2], J. Hobirk[7], A. Huber[3], S. Jachmich[8], E. Joffrin[1], H.R. Koslowski[3], Y. Liang[3], Th. Loarer[1], P. Lomas[2], T. Luce[9], J. Mailloux[2], G.F. Matthews[2], K. McCormick[7], D. Mazon[1], D. Moreau[1], V. Pericoli[4], V. Philipps[3], E. Rachlew[10], S.D.A Reyes-Cortes[11], G. Saibene[12], S. E. Sharapov[2], I. Voitsekovitch[2], L Zabeo[2], O. Zimmermann[3], K.D. Zastrow[2] and the JET-EFDA contributors*

*JET-EFDA Culham Science Centre, OX14 3DB, Abingdon, UK*
*[1] Association Euratom-CEA, CEA/DSM/DRFC-Cadarache 13108, St Paul Durance, France*
*[2] Euratom/UKAEA Fusion Association, Culham Science Centre, Abingdon, Oxon OX14 3DB UK*
*[3] Forschungszentrum Jülich GmbH, Institut für Energieforschung-Plasmaphysik, EURATOM-Assoziation, Trilateral Euregio Cluster, D-52425 Jülich, Germany*
*[4] Associazione Euratom-ENEA, ENEA Centro Ricerche Frascati C.P. 65, 00044 Italy*
*[5] Association Euratom-Confédération Suisse CRPP EPFL 1015 Lausanne Switzerland*
*[6] Asociacion Euratom-CIEMAT, ES Avenida Complutense 22 E-28040 Madrid Spain*
*[7] Association EURATOM-Max-Planck-Institut für Plasmaphysik, D-85748 Garching, Germany*
*[8] Association EURATOM-Belgian State, ERM/KMS, Brussels, Belgium*
*[9] General Atomics, PO Box 85608, San Diego, CA 92186-5608, USA*
*[10] Association Euratom-VR, Dept. Phys., KTH, SE 10378, Stockholm Sweden*
*[11] Centro de Fusão Nuclear, Associação Euratom-IST, Instituto Superior Técnico, 1049-001 Lisboa, Portugal*
*[12] EFDA Close Support Unit, Boltzmannstr. 2, 85748 Garching, Germany*
** See annex of M.L. Watkins et al, "Overview of JET Results ", (Proc. 21st IAEA Fusion Energy Conference, Chengdu, China (2006)).*

Preprint of Paper to be submitted for publication in
Plasma Physics and Controlled Fusion

**ABSTRACT**

A key issue for steady-state tokamak operation is to determine the edge conditions that are compatible both with good core confinement and with the power handling and plasma exhaust capabilities of the Plasma Facing Components (PFCs) and divertor systems. A quantitative response to this open question will provide a robust scientific basis for reliable extrapolation of present regimes to an ITER compatible steady-state scenario. In this context, the JET programme addressing steady-state operation is focused on the development of highly non-inductive, high confinement plasmas with the constraints imposed by the PFCs. A new beryllium main chamber wall and tungsten divertor together with an upgrade of the heating/fuelling capability are currently in preparation at JET. Operation at higher power with this ITER-like wall will impose new constraints on non-inductive scenarios. Recent experiments have focused on the preparation for this new phase of JET operation. In this paper, progress in the development of Advanced Tokamak (AT) scenarios at JET is reviewed keeping this long-term objective in mind. The approach has consisted of addressing various critical issues separately during the 2006-2007 campaigns with a view to full scenario integration when the JET upgrades are complete. Regimes with Internal Transport Barriers (ITBs) have been developed at $q_{95}$~5 and high triangularity, $\delta$ (relevant to the ITER steady-state demonstration) by applying more than 30MW of additional heating power reaching $\beta_N$~2 at $B_0$~3.1T. Operating at higher $\delta$ has allowed the edge pedestal and core densities to be increased pushing the ion temperature closer to that of the electrons. Although not yet fully integrated into a performance enhancing ITB scenario, Neon seeding has been successfully explored to increase the radiated power fraction (up to 60%), providing significant reduction of target tile power fluxes (and hence temperatures) and mitigation of Edge Localised Mode (ELM) activity. At reduced toroidal magnetic field strength, high $\beta_N$ regimes have been achieved and q-profile optimisation investigated for use in steady-state scenarios. Values of $\beta_N$ above the 'no-wall MagnetoHydroDynamic (MHD) limit' ($\beta_N$~3.0) have been sustained for a resistive time in high-$\delta$ configurations (at 1.2MA/1.8T). In this scenario, ELM activity has been mitigated by applying magnetic perturbations using error field correction coils to provide ergodisation of the magnetic field at the plasma edge. In a highly shaped, quasi-double null X-point configuration, ITBs have been generated on the ion heat transport channel and combined with 'grassy' ELMs with ~30MW of applied heating power (at 1.2MA/2.7T, $q_{95}$~7). Advanced algorithms and system identification procedures have been developed with a view to developing simultaneously temperature and q-profile control in real-time. These techniques have so far been applied to the control the q-profile evolution in JET advanced tokamak scenarios.

**INTRODUCTION**

Efficient operation of a steady-state thermonuclear fusion reactor based on the tokamak concept requires the simultaneous optimisation of:

(i) the fusion gain, measured by the ratio of fusion power to the additional heating and current drive power externally applied, $Q_{DT}$; and

(ii) the self-generated non-inductive bootstrap current, driven internally by the plasma pressure gradients, to minimise the current that must be driven by external power sources.

Optimisation of these quantities leads to a tokamak operational domain with high normalised plasma pressures, $\beta_t$ and $\beta_p$, where respectively the plasma pressure is normalised to the toroidal magnetic field pressure to maximise $Q_{DT}$, and to the poloidal magnetic field pressure to maximise the bootstrap current fraction. Since the product of $\beta_t \times \beta_p$ is proportional to $\beta_N^2$ (defined as $\beta_N = \beta_t (Ip/aB_o)$-1, where $\beta_t$ in %, a is the minor radius in m; $B_o$ is the on-axis toroidal magnetic field in T; and $I_p$ is the plasma current in MA), steady-state reactor operation will be at high $\beta_N$ values typically above the usual values imposed by the MHD no-wall limit [40]. Operation of a tokamak at high $\beta_N$ is challenging, commonly referred to as advanced tokamak (AT) operation, and typically requires the use of highly shaped plasmas and active control of the pressure and current density profiles. This permits improved thermal confinement and stability, together with the stabilisation of resistive wall modes that is required to significantly exceed the no-wall stability limit (e.g. as recently reviewed in [9](a), [20](a)).

Demonstration of steady-state tokamak operation at high $Q_{DT}$ is one of the ITER objectives. Fully non-inductive operation (i.e. without transformer flux consumption) is envisaged for up to 3000s with $Q_{DT}$~5 and a bootstrap current fraction ($I_{bootstrap}/I_P$) typically above 50% at a normalised beta of the order of $\beta_N$~2.9 ([20], [23]). The part of the plasma current not driven by the bootstrap effect must be generated by external means. To minimise the power required by these external sources it is foreseen that the plasma current would be reduced down to 9MA, corresponding to a safety factor at 95% of the poloidal flux, $q_{95}$, of around 5. The magnetic configuration would be characterised by a triangularity at the separatrix, $\delta_x$, of order 0.5 and an elongation of $\kappa_x$~2. To compensate for the reduction in energy confinement normally expected when reducing the plasma current from the nominal value of 15MA down to 9MA, the ITER steady-state regime must achieve improved confinement as quantified by the quality factor, $H_{IPB98(y,2)}$, obtained by normalising the thermal confinement time to that predicted for the Type I ELMy H-mode reference scenario (ITER Physics Expert Groups 1999). An improvement factor of $H_{IBP98(y,2)}$~1.5 is required simultaneously with a high absolute density ($n_l$~6.5x$10^{19}$$m^{-3}$) corresponding in turn to a high density normalised to the Greenwald density, $n_l/n_{Gw}$~0.8 where $n_{Gw}=I_p/(\pi a^2)$. Achievement of higher confinement compared to the ELMy H-mode scaling relies on the combination of an edge transport barrier (as obtained in†H-mode) with an ITB as recently reviewed [41]. In addition, fusion performance optimisation in steady-state should be obtained in conditions compatible with the ITER Plasma-Facing Components (PFCs). In the present ITER design a beryllium first wall with castellated tungsten tiles at the divertor baffle and dome and castelled tiles of Carbon Fibre Composite (CFC) at the divertor strike points are foreseen ([43],[36], [17], [33], [35] (c.f. Fig. 1). In ITER, parallel heat fluxes in the SOL will reach ~1$GWm^{-2}$ [43]. To satisfy the technological constraints imposed by the divertor target PFCs, this parallel heat flux must be reduced to a perpendicular load of typically 10 $MWm^{-2}$ in steady-state and up to 20

$MWm^{-2}$ for transient loads. This is only possible in ITER if the partially detached divertor (at the outer strike point) condition is achieved – a condition which is in fact the reference regime for ITER divertor operation [34]. In a partially detached divertor, perpendicular heat fluxes in the strike point regions (where the parallel fluxes are highest) are considerably reduced, principally as a consequence of local ion-electron recombination promoted by the very low plasma temperatures and higher densities in the divertor volume. Such conditions are achieved by optimising divertor design to increase neutral pressures (enhancing ion-neutral charge-exchange momentum loss) and enhance local radiation loss. In ITER, the latter will require further enhancement (over that occurring naturally due to hydrogenic and impurity radiation) via the use of extrinsic seeding, typically using noble gas impurities. This is especially true if the high densities that are required in the divertor for recombination to be effective cannot be naturally achieved, as may be the case for advanced scenarios which typically operate at lower edge densities [55].

Optimising the fusion performance with the constraints imposed by the ITER PFCs is an important issue and challenge that will be addressed on JET to provide timely preparation of the ITER scenarios. A new beryllium wall in the main chamber and a tungsten divertor (with tungsten coated CFC at the inner divertor leg and bulk tungsten on the outer divertor leg) will be installed on JET [49] together with an upgrade of the heating and fuelling capability. Operation with this new ITER-Like Wall (ILW) at high power will set new constraints on non-inductive scenarios that need to be properly identified. In particular, without carbon in the machine and with higher available heating power, extrinsic impurities will be required to promote the high radiation levels required to maintain tolerable divertor target heat loads and to reduce the plasma temperatures at the targets sufficiently to avoid strong physical sputtering of tungsten. One of the main themes of the recent (2006-2007) AT experimental campaign on JET has been to begin the development of advanced scenarios that could be made compatible with the future beryllium wall and tungsten divertor.

After this introduction, the paper is organised as follow:

- in section 2, the issues related to plasma operation with a metallic wall are briefly presented;
- in section 3, a summary of the progress achieved in advanced scenarios at $q_{95}$~5 with ITER-like magnetic configuration in the 2006-2007 experimental campaign is given;
- in section 4, the different approaches developed at JET for edge control of advanced regimes are discussed in detail, in particular using increased radiation in the divertor, optimising the plasma shape, and ergodising the magnetic field at the plasma edge;
- finally, in section 5, conclusions are drawn with the emphasis on future progress that is needed.

## 2. STEADY-STATE SCENARIOS AND WALL COMPATIBILITY

Fully non-inductive operation, in particular at high density, requires an extension of the heating, current drive and fuelling capability of the JET device. Therefore, in addition to the installation of the new PFCs as previously described in the introduction (c.f. Fig.1), the tools for the long-term JET programme in preparation of ITER operation are: an ITER-like Ion Cyclotron Resonance

Heating (ICRH) antenna designed to be resilient to fast varying loads due to ELMs and to deliver an additional ~7MW at a power density of 8MW/$m^2$ in a wide frequency range of 30-55MHz; an upgrade of the Neutral Beam Injection (NBI) power to 35MW/20s or 17.5MW/40s (compared with ~25MW/10s or ~12MW/20s at present); a new pellet injector for ELM control; and improved diagnostic and control capability [50], [15], [10], [19]. With this increased heating power capability (up to 45MW) simulations indicate that the operational space of JET non-inductive regimes can be extended in terms of plasma current (reaching $I_p$~2.5MA) and density ($n_l$>5x$10^{19}m^{-3}$), with high $\beta_N$ ($\beta_N$>3.0) and a bootstrap fraction of 60-70% at high toroidal magnetic field (~3.5T) and $q_{95}$~5 [42]. These performance figures could be reached if a confinement enhancement factor of up to $H_{IPB98(y,2)}$~1.5 is sustained at 45MW. Even though the current ITER materials choice [43] has CFC at the target plates (essentially for power handling purposes), the planned JET ILW will begin with all-W divertor targets [49], [44], in an attempt to study the degree of reduction in the critical problem of tritium retention in the absence of carbon. At the same time, the all-metal wall will provide a severe challenge to scenario development, allowing JET the invaluable opportunity to test ITER relevant AT regimes at high power and to develop strategies for coping with the demands of metal targets (which are considered essential for fusion reactors in the long term). If such tests prove successful, they are likely to have a strong influence on the eventual choice of first wall material mix that will be used for burning plasma operation in ITER.

The removal of carbon and its replacement with tungsten at the divertor targets and beryllium on the first wall forces the AT scenario developer to account for a number of issues related to plasma-wall interaction, such as:

- melting of W and Be should be avoided, or at least, minimised;
- there is no chemical sputtering in the absence of carbon, but tungsten physical sputtering (self-sputtering and impurity sputtering) should be minimised;
- core plasma contamination (e.g. impurity accumulation) of high-Z ions, such as tungsten, should be avoided to optimise the fusion performance;
- carbon is a powerful radiator in the temperature range typical of the divertor plasma – in its absence, impurity seeding will be required; in turn, these impurities must be carefully controlled to avoid heavy ion sputtering of the W targets and to maintain the radiation at the required levels without excessive core accumulation.

These new constraints will require the development of plasma scenarios that provide acceptable energy and power loads to the PFCs by minimising:

(i) transient (e.g. due to ELMs, plasma disruptions, etc.) and stationary heat loads;
(ii) NBI losses on the main chamber walls at reduced plasma density due to the shine-through effects;
(iii) fast ions losses (e.g. generated by NBI or ICRH power) and fast electron losses (e.g. generated by LHCD or after a disruption) on the PFCs.

Ultimately, optimisation of the energy and power load on the PFCs must be achieved without compromising the plasma fusion performance. The source of tungsten at the plasma edge should be minimised together with core plasma impurity concentration while increasing the plasma thermal energy (and particle) confinement and MHD stability with respect to standard inductive ELMy H-mode operation. For steady-state regimes these constraints provide important challenges that must be addressed in present-day experiments. Such regimes should operate simultaneously:

(i) at high edge (and core) density and low edge temperature;
(ii) with 'mild' ELM activity;
(iii) with a high level of radiated power in the divertor;
(iv) without the deleterious effects of impurity accumulation in the core but, nevertheless, with improved energy confinement.

This paper reports on the results of experiments at JET devoted to the characterization and optimisation of edge conditions in steady-state scenarios with a view to integrating the constraints imposed by the future metallic wall.

## 3. OVERVIEW OF THE JET PERFORMANCE WITH ITER-LIKE MAGNETIC CONFIGURATION

In order to begin the preparations for advanced scenario operation on JET in the context of the coming power upgrade and PFC changes, a major effort has been devoted in the 2006-2007 experimental campaign to operate at high plasma triangularity and relevant $q_{95}$~5 for advanced scenarios, at higher core and edge density and at high values of normalised pressure ($\beta_t$ or $\beta_p$).

During the 2004-2005 shutdown the installation of the new MKII-HD divertor with a new Load-Bearing Septum Replacement Plate (LBSRP) made of CFC offers more freedom in the choice of configuration and provides access to higher triangularity at higher plasma current. The standard magnetic configuration commonly used in the past to develop high performance plasmas with core ITBs is characterized by low values of (upper and lower) triangularity with the strike points located in corners of the divertor offering efficient pumping (Fig.2). To develop magnetic configurations with ITER-like plasma shape (named ITER-AT), the outer strike point is moved inwards towards the LBSRP, the inner strike point is moved upwards and the X-point position is pushed closer to the inner wall (Fig. 2). Such configurations reach values of lower triangularity at the separatrix, $\delta_l$, up to ~0.55, and upper triangularity, $\delta_u$, up to ~ 0.45. In the course of the optimization several plasma shape parameters have been varied, such as: (i) the X-point position relative to the inner wall proximity; (ii) the inner and outer strike point positions to optimize diagnostic coverage in the divertor (e.g. thermocouples, Langmuir probes, spectroscopy, etc.) or pumping efficiency for edge density control; and, finally, (iii) the values of upper and/or lower triangularity. For example, an intermediate configuration between the low triangularity and ITER-like configurations is the so-called LUD (Lower Upper Delta) with similar values of upper triangularity to the previous low

triangularity cases (i.e. $\delta_u$~0.3) while having $\delta_l$~0.55.

To demonstrate the progress made at different values of toroidal magnetic field in terms of normalized fusion performance measured by the figure of merit, $\beta_N$, discharges with $\delta_l \geq 0.35$, $4 \leq q_{95} \leq 6$ and a duration of the high performance phase sustained for at least ten energy confinement times have been selected from the EFDA-JET database (2000-2007). The results are summarized in Fig. 3 where $\beta_N$ values are plotted versus the total input power (each point corresponds to one discharge). Past results in terms of the development of high $\beta_N$ regimes for steady-state applications have recently been summarized in [21] and are briefly recalled here:

- In 1995, plasmas with $\beta_N$ values up to ~3.8 (1.4MA/1.4T) were sustained for 1s, but without any attempt to optimize the q-profile shape, i.e. starting with standard inductive q-profiles, which are not compatible with a large fraction of non-inductive bootstrap current in steady conditions [6];
- In 1999, plasmas with $\beta_N$~2.6 were developed with an optimized shear q-profile (i.e. with 'weak' central magnetic shear) and with an ITB, but at low triangularity [22];
- In 2000-2004, first attempts to develop scenarios with improved core confinement at high triangularity were made with optimized q-profiles [13], [56], [53].

As shown in Fig.3, major progress in operation at high power and/or high $\beta_N$ values in configurations relevant to ITER steady-state operation has been made during the 2006-2007 JET campaigns. The results obtained can be summarized as follows:

- At $B_o$~3T (typically at $I_p$~1.9MA, $q_{95}$~5) most of the plasma shape and scenario development has been done in order to be far from the MHD stability limits. In this case the applied power has been maximized up to 32MW (combining the NBI, ICRH and LHCD powers) with $\beta_N$ up to 2.1;
- At $B_o$~2.7T ($I_p$~1.2-1.5MA) successful attempts have been made to develop a quasi-double-null plasma shape with the objective to obtain a regime where ITBs are combined with grassy ELMs as defined in [54] at high poloidal beta ($\beta_p \geq 1.6$), approaching the relevant $q_{95}$ values for ITER steady-state operation. This ELMs regime was also obtained in JT-60U when $\beta_p$ exceeds 1.6-1.7 [31];
- At $B_o$~2.3T ($I_p$~1.5MA) efforts have been made to develop ITB regimes at high $\beta_N$ with small amplitude Type I ELMs or Type III ELMs [47], [5]. Discharges with $\beta_N$ up to 2.8 have been sustained for 8 confinement times with an ITB in the ion heat channel at mid-radius and with up to 30MW of additional heating power [47], [48], [11], [24];
- At $B_o$~1.8T ($I_p$~1.2MA) the objective was to sustain plasmas close to or above the no-wall limit to study the conditions for optimizing plasma stability in the case of weak, or even without, improved core confinement. In regimes with good edge confinement and Type I ELMs, $\beta_N$ values of ~3.0 (above the no-wall limit) have been sustained for a resistive time (~7s) with ~ 15MW of NBI power [9], [24].

It should be stressed that, in this database at high triangularity, the improved confinement factor relative to the ELMy H-mode scaling, $H_{IBP98(y,2)}$, does not exceed 1.1 since either: (i) the edge confinement has the characteristics of the standard Type I ELM regime without improved core confinement; or (ii) the edge pedestal is degraded (e.g. in the Type III ELM regimes with gas puffing) and the improved core confinement serves to compensate for the degradation of the edge transport barrier.

Regimes at high triangularity naturally provide access to high density operation compared with standard low triangularity configurations. This is illustrated on Fig.4 (left) where the electron temperatures are plotted versus the electron density at the top of the H-mode pedestal measured by Thomson scattering for the three typical configurations: (i) low triangularity; (ii) LUD; and (iii) ITER-AT (c.f. Fig.2). The high triangularity configurations typically have $N_{e\text{-}ped}\sim3\times10^{19}m^{-3}$ with $T_{e\text{-}ped}\sim1.2$keV and clearly occupy a different domain in this diagram compared with the low triangularity cases characterized by $N_{e\text{-}ped}\sim1.75\times10^{19}m^{-3}$ and $T_{e\text{-}ped}\sim1.5$keV. It is worth noting that both the LUD and the ITER-AT configurations have essentially the same pedestal parameters, suggesting that the lower magnetic configuration (i.e. at the divertor) is important for the edge MHD stability (the critical parameter could, for example, be the lower triangularity and/or the proximity of the X-point to the inner divertor target tiles). As shown in Fig. 4 (right), access to higher density at the top of the pedestal is a possible route for the development of high core density plasmas where the density normalized to the Greenwald density has reached $n_l/n_{Gw}\sim0.8$ at $\beta_N\sim2.5$, approaching simultaneously the values envisaged for ITER.

High $\beta_N$ (up to ~ 2.8) regimes with improved confinement through the generation of ITBs, characterized by high values of normalised ion temperature gradient $R/L_{Ti}$ (where $L_{Ti}=T_i/\nabla T_i$ and $\nabla$ Ti is the ion temperature gradient estimated at mid-plasma radius, R is the major radius at this location in the outer mid-plane) have been sustained for eight confinement times (but shorter than the resistive time). Fig.5 shows $\beta_N$ versus $R/L_{Ti}$ for various toroidal magnetic fields indicating that $R/L_{Ti}\geq15$ has been reached at $\beta_N\sim$ 2.8. The limitation in duration is thought to be due to a slow evolution of the current density profile leading to core MHD instabilities [11], [48], [47]. Ultimately, sustaining very high $\beta_N$ values on a resistive time will require active plasma profile control with a higher fraction of non-inductive current, in addition to the control of the global parameters (e.g. $\beta_N$ control), either using q-profile control alone or in combination with pressure profile control. In this context a major effort has been made at JET to develop a sophisticated control system that uses the combination of the heating and current drive systems and, optionally, the poloidal field system, in an optimal way to regulate the evolution of several pressure and current profile parameters [45], [46], [3]. Control of the q-profile has been performed at high toroidal magnetic field and reduced $\beta_N$ values ($B_o\sim3$T, $I_p\sim1.1$-1.5MA, LUD magnetic configuration). The control phase lasted more than 7s using the three heating and current drive systems while separately requesting constant loop voltage. Eventually, control was attempted using four actuators in a single controller, including the loop voltage. This work provides an important step in validating the integrated methodology for controlling the q

profile, although some improvements are needed for the practical use of the ohmic drive (poloidal field system and plasma shape controller) as an additional actuator. These control systems must also be further developed and tested for application to regimes close to operational limits.

## 4. EDGE CONTROL FOR JET ADVANCED MODES OF OPERATION

As a first step towards the ultimate goal of developing high power, steady-state scenarios compatible with the future choice of PFCs on JET, various approaches for controlling the edge conditions have been attempted:

(i) increasing the radiation power by impurity seeding in the divertor to reduce the target heat flux;
(ii) optimising the plasma shape (e.g. with a quasi-double-null magnetic configuration to mitigate the ELM behaviour or with divertor strike point 'sweeping' to spread the target heat flux);
(iii) ergodising the magnetic field lines in the vicinity of the plasma separatrix to reduce the ELM perturbation.

These approaches are described in more detail in the following subsections.

### *4.1 RADIATIVE DIVERTOR*

The high triangularity advanced tokamak scenario on JET usually consists of applying Lower Hybrid Current Drive (LHCD) power during the plasma current ramp-up phase together with an early transition to a highly shaped X-point plasma. Thanks to the electron heating and off-axis nature of the LH current source, it has been demonstrated in past experiments at low δ that a wide variety of broad q-profiles have been obtained at the end of the prelude phase[7], [8]. High power NBI and ICRH are then applied in two or three steps when the required q-profile has been obtained to provide the necessary stability and confinement. Lower Hybrid power is usually maintained during the high power phase to sustain the required q-profile, together with a combination of bootstrap, neutral beam and the remaining ohmic current. In the example shown in Fig. 6 (left), corresponding to a LUD configuration at 1.9MA/3.1T and $q_{95}$~5, deuterium gas was injected to obtain high frequency Type I ELMs (f~100-80Hz) with about 30% of the input power being radiated (mainly by Carbon) and $N_{e\text{-}ped}$~2.5-2.8×$10^{19}m^{-3}$ with $T_{e\text{-}ped}$~1.1-1.3keV. The radiated power is measured with the vertical bolometer camera and the value between ELMs is systematically used in this paper. With this high edge (and core) density compared to low d experiments a weak ITB was seen as a steepening of the gradient of the ion temperature profile at mid-radius from t~5s with similar values for the ion and electron temperature (no clear sign of an ITB was seen on the electron temperature profile).

With a similar magnetic configuration and high power heating the radiated power fraction ($P_{rad}$/$P_{tot}$) has been increased from 30% up to 55% by injecting neon gas in the divertor region between

t=4s and t=8s, as illustrated in Fig.6 (right). Spectroscopic analysis shows, that the amount of injected neon was not sufficient to replace carbon completely as radiator in the divertor. With increasing $P_{rad}/P_{tot}$ the Type I ELMs become more frequent with low amplitude and, as a consequence, the radio-frequency systems are more readily able to couple power to the plasmas. For the discharge shown in Fig.6 (right) about 31-32MW of total power was applied, consisting of ~20MW of NBI, ~8MW of ICRH and ~3.5MW of LHCD, with up to 17MW was radiated, mainly in the divertor region. At 1.9MA/3.1T, the normalised beta reached $\beta_N$~2 and the diamagnetic stored energy was $W_{dia}$~5.6MJ. It should be noted that 0.5s after the neon injection was switched-off the ELMs became large, similar to those seen in the standard Type I ELM regime.

A specific set of experiments have been designedin which $P_{rad}/P_{tot}$ has been systematically increased using different amounts of neon seeding (Beurskens et al 2007). The reference discharges at $P_{tot}$~20-25MW without any fuelling have $P_{rad}/P_{tot}$~15% with low frequency Type I ELMs, typically below 50Hz and with $\Delta W_{dia}/W_{dia}$~6%. Two optimum regimes, in terms of the normalised plasma energy drop per ELM, $\Delta W_{dia}/W_{dia}$, were found with neon injection corresponding to:

(i) $P_{rad}/P_{tot}$~30%, with high frequency Type I ELMs, typically above 100Hz leading to $\Delta W_{dia}/W_{dia}$ <2%;

(ii) $P_{rad}/P_{tot}\geq$50% with either Type III ELM behaviour ($\Delta W_{dia}/W_{dia}$<2%), or even with an L-mode edge.

The two discharges shown in Fig. 6 illustrate the ELM behaviour for these two operational regimes. Finally, the intermediate domain at $P_{rad}/P_{tot}$~40% has to be avoided since it corresponds to a regime of compound ELMs with large and low frequency type I ELMs.

To better investigate the effect of core dilution and impurity accumulation, the high power pulse duration was extended to 6s at 30MW power level, approximately corresponding to the maximum allowed duration using the ITER-AT magnetic configuration due to engineering constraints. Fig. 7 shows similar pulses, in terms of applied power and configuration at $B_o$=3.1T/$I_P$=1.9MA, but with different levels of neon seeding. The neon was injected only between t=5s and t=9s. When increasing the neon seeding (Pulse No: 69093), the amplitude of the ELM perturbation was strongly reduced (with the exception of the first ELMs at around t=5s) and the diamagnetic stored energy was also increased by 25%. This performance improvement is seen on the ion temperature profiles which show a temperature increase both at the top of the H-mode pedestal and in the core (from 6keV to 12keV) with the electron density also increasing by ~10% in the core. The cause of the improvement has not yet been identified but could have similar origin to previous experiments in TEXTOR, JET and DIII-D with argon seeding[59], [15] [28]. The neon concentration profile, as measured by the charge exchange recombination spectroscopy, is hollow with a concentration of about 1% in the core rising to ~2.5% at a normalised radius of 0.7. Analysis from a wider database has also confirmed that no sign of impurity accumulation is found in these discharges. However, it should be noted that these experiments do not have very steep internal gradients in either the temperature or density

profiles. This is in contrast to previous experiments with strong internal transport barriers, which have led to impurity accumulation and even radiative collapse in the core [16]. Nevertheless, the consequences, in terms of core impurity content, when increasing the radiated power with neon at to $P_{rad}/P_{tot}$~50% are the following:

(i) an increase of the line averaged effective charge, $Z_{eff}$, from 1.5 to 2.5;
(ii) a reduction of $n_D/n_e$ from 90% to 80% where $n_D$ is the deuterium density;
(iii) a reduction of the carbon concentration down from ~3% to ~1% (at r/a~0.6);
(iv) a reduction in the electron pedestal pressure of between 20-30%.

All these effects lead to a reduction in the fusion performance. At high radiated power fraction (above 50%) an improvement of core confinement is required to recover the reduction in performance due to the impurity seeding. In Fig. 8 the measured neutron yield (which is mainly due to beam-target reactions) is plotted versus the radiated power for a narrow range of applied powers and densities. It indicates that some discharges (as also seen in the time traces of Fig. 7) can have the same neutron rate at $P_{rad}/P_{tot}$~50% as at $P_{rad}/P_{tot}$~20%.

Detailed power balance analysis for these plasmas in the ITER-AT magnetic configuration [4], 27] indicates that 80% of the conducted power crossing the separatrix is deposited in the divertor region, as deduced from divertor target tile thermocouple measurements. Wide angle, main chamber Infra-Red (IR) camera measurements meanwhile show that ~10% is deposited on the dump-plates at the top of the main chamber. Figure 9 shows a wide angle IR image of the JET in-vessel PFCs using the new IR system, which has been designed using ITER relevant reflective optics [18] , [2]. The white areas denote the hottest components and clearly illustrate the main plasma-wall interaction in the divertor (bottom) and the upper dump plate (above the plasma). The bright spots localised around the outboard mid-plane indicate interactions induced by ICRH heating on the septum parts of the antennas [12]. Since most of the power crossing the separatrix is deposited in the lower divertor, an effort has been made to measure the deposited energy distribution at the target tiles with different levels of neon injection and radiated power. The results are summarised in Fig.10 (left) where the energy measured by thermocouples uniformly distributed in the various divertor tiles is plotted versus the tile number for four levels of $P_{rad}/P_{tot}$. Fig.10 (left) indicates that when $P_{rad}/P_{tot}$ is increased the energy deposition profile is more uniformly distributed. In particular the energy on the LBSRP (tile 5), at the outer divertor strike point, is reduced by more than a factor of 2 and the tile temperature remains below 400$^{o}$C [4]. In contrast, the energy flowing to the inner divertor strike point on tile 1 is only slightly reduced when increasing the ratio $P_{rad}/P_{tot}$. This is almost certainly due to the short length of inner leg (i.e. the distance between the strike-point position and X-point along the magnetic separatrix). Such short distances do not allow sufficient residence time for particles to lose energy during their transport to the strike regions. In addition, the lack of divertor baffling on the inboard side does not permit the build up of high neutral densities, facilitating local plasma cooling.

The electron temperature in the outer strike point region has also been measured with divertor Langmuir probes located on the LBSRP close to the outer divertor strike point (tile 5) [27]. As shown in Fig.10 (right), the edge electron temperatures between ELMs and at the ELM peaks are significantly reduced when increasing $P_{rad}/P_{tot}$ to a level of 50%, with reductions of a factor four and two respectively. It can bee seen that the edge electron temperature between ELMs could be reduced below 10eV at $P_{rad}/P_{tot}$~50%.

Finally, gas injection valves located at different places on the JET vessel (i.e. different poloidal locations in the divertor or main chamber) have been used to inject neon impurities. The radiation pattern is found to be nearly independent of the injection location with around 90% of the radiated power originating outside the magnetic separatrix in the divertor region. Fig.11 shows the radiation pattern as deduced from the newly installed bolometer camera for four discharges with different levels of neon injection and $P_{rad}/P_{tot}$ (Huber et al 2007). It indicates that the radiation pattern is spatially localised and, when $P_{rad}/P_{tot}$ is increased, that the radiation level is mainly increased at the inboard side and around the X-point location.

### *4.2 SHAPE OPTIMISATION*

The first approach to shape optimisation for wall compatibility has been to develop sweeping techniques to vary in time the location of the strike points on the divertor tiles to share the power load between the various surfaces [56]. This possibility has been recently enhanced by the new plasma shape control scheme provided by the extreme shape controller enhancement [51], [58] [1]. This sweeping technique was successfully tested in a 20s long pulse to extend the duration of the hybrid regime at $I_p$~1.3MA, $B_o$~1.5T, $q_{95}$~3.5 and NBI power levels around 10MW [58], [30]. The divertor strike points have been swept with a peak to peak amplitude of 7cm and a frequency of 4Hz with no significant confinement losses and only a slight influence on the ELM frequency. The local temperature at the divertor target tile has been measured with the new infrared camera, showing that sweeping causes a decrease of the maximum surface temperature on the tile at outer divertor strike point of about $100^{o}$C.

The second approach was to develop ITB regimes with grassy ELMs as defined in [54], exploiting a quasi-double-null magnetic configuration where the q-profile was tailored during the ramp-up phase with the application of LHCD power, as routinely done in JET advanced scenarios. In previous experiment to develop this ELM regime prior to the 2006 experimental campaign, QDN shapes were only used in the inductive ELMy H-mode regime without any attempts to optimise the q-profile above unity for steady-state application. The experiments described in this paper have been performed at a toroidal magnetic field strength of 2.7T with $q_{95}$ ranging from 5 to 7. An overview of the results is shown in Fig.12 (left) where the poloidal beta has been plotted versus the additional heating power. The filled symbols correspond to cases where an ITB was detected from the ion temperature profile using the criteria as defined in [57]. The figure indicates that a power level above 20MW was required to obtain an ITB for this set of experiments. It was found that the grassy

ELM regime, where there is no correlation between the ELM crashes and the variation in the energy diamagnetic content, was reached in the quasi-double-null configuration at: low internal inductance, $l_i$ (~0.8-0.9); high $\beta_p$ (≥1.6), $q_{95}$ in the range from 5.8 to 7; and at high normalised electron collisionality ($n_e$*~0.3-0.6). The domain where ITBs (with $P_{tot}$>20MW) and grassy ELMs ($\beta_p$≥1.6) were simultaneously achieved is highlighted in Fig. 12 (left). At this magnetic field, high power (above 31MW) is required to reach the domain where the poloidal beta is above 1.6 at ITER relevant $q_{95}$~5. Typical time traces of a high power pulse (21MW of NBI and 9MW of ICRH power during the high power phase, while 2MW of LHCD is applied in the prelude phase) at Ip~1.35MA, $B_o$~2.7T and $q_{95}$~6 are shown in Fig.12 (right) where a transition to a grassy ELM regime, leading to a reduction of the ELM amplitude on the $D_\alpha$ signal measured in the divertor, is observed when $\beta_p$ values are maintained above 1.6.

### *4.3 EDGEMAGNETICFIELD ERGODISATION*

Another approach that has been used to mitigate the ELMs in JET advanced scenarios is to induce an edge magnetic field perturbation using the error field correction coils, [38], [39] [32]. This method, initially exploited on JET in the standard ELMy H-mode regime, has also been successfully applied in the high triangularity advanced tokamak scenarios at high $\beta_N$, but at reduced toroidal magnetic field ($B_o$~1.8T, Ip~1.3MA, $q_{95}$~4.5). The EFCCs were energised in an n=1 mode, where n is the toroidal mode number, to provide a weak edge ergodisation of the magnetic field line. Fig. 13 shows one example of such a discharge where the EFCC perturbation was applied between t=5s and t=7.5s. The NBI power was feedback controlled to maintain a prescribed $\beta_N$ value of 2.5. Prior to the application of the perturbation induced by the EFCCs, the ELMs have the standard Type I characteristics with an edge transport barrier that provides a normalised thermal confinement of $H_{IPB98(y,2)}$~1. During the application of the EFCC perturbation, the ELM amplitude was significantly reduced, leading to an ELM energy loss below 2% of the total stored energy. During this phase the density at the top of the H-mode pedestal decreased by 20%, but the global thermal confinement factor, $H_{IPB98(y,2)}$ remained constant around unity. This observation is explained by an increase of the core (ion and electron) temperature, which led to a higher core energy that compensated for the reduction of the pedestal energy. This technique was successfully applied in similar regimes with $\beta_N$ up to 2.9, but further technical development will be required to increase the pulse duration capability of EFCC system at the required large coil currents.

## DISCUSSION, CONCLUSION AND PROSPECTS

During the 2006-2007 experimental campaign significant progress has been made at JET towards the development of reliable advanced tokamak scenarios, which can be summarised as follow:

- Regimes have been extended at high power (above 30MW) with an ITER relevant plasma shape (triangularity and elongation) and $q_{95}$~5 with a q-profile optimised for steady-state application;

- Regimes have been explored at higher density in both the plasma edge and core compared to the previous values obtained in low triangularity experiments, with $T_i$ close to $T_e$;
- At reduced toroidal magnetic field (2.3T or 1.8T) MHD stability has been explored at the ITER relevant plasma shape and $q_{95}$; $\beta_N$ values of the order of 3 have been sustained above the no-wall limit for a resistive time (~7s) but without a significant ITB; In the presence of an ITB on the ion heat channel $\beta_N \sim 2.8$ has been sustained for eight confinement times, with the duration being limited by the q-profile evolution;
- Advanced control techniques have been developed that integrate the real-time control of the plasma shape and the magnetic/kinetic profiles. These techniques have been used to control the q-profile with three actuators and a prescribed loop voltage.

An ongoing effort has also been devoted to the specification of conditions for advanced scenarios that would be compatible with the constraints imposed by the upgrade to the plasma facing components on JET, i.e. the ITER-like wall project. This project consist of the replacement of the present CFC components by a Be main chamber wall and a W divertor. Operation with this new ITER-like wall at high power will set new constraints on non-inductive scenarios that has been identified in present experiments. In this context, experimental effort has been devoted to the characterization of the plasma edge of the advanced scenarios and the development of regimes that could be made compatible with the future Be and W components. During the 2006-2007 experimental campaign, different approaches have been pursued with the aim of optimizing an integrated scenario compatible with the future metallic wall, which are summarized as follow:

- By injecting high-Z radiative gas, such as neon, to increase the edge radiation. This approach usually leads to high radiated power fraction (typically around 50%) with a decrease of the confinement performance of the edge (H-mode) transport barrier. A significant enhancement of the core confinement is therefore required to compensate for the edge pedestal degradation and the plasma current reduction ($q_{95}$~5) to ultimately operate in fully non-inductive conditions. Two regimes with mild ELM activity have been found at either $P_{rad}/P_{tot}$~30%, with high frequency Type I ELMs, or at $P_{rad}/P_{tot} \geq 50\%$, with Type III ELMs or an L-mode edge. It is not obvious that the first regime at $P_{rad}/P_{tot}$~30% could be directly translated to future experiments with the new ITER-like wall since the radiation level is mainly determined by carbon. Regimes at $P_{rad}/P_{tot} \geq 50\%$ usually require higher core confinement to compensate for the reduction of pedestal energy.
- By sweeping the strike points to spread the heat load on the divertor tiles. Since the PFCs are not actively cooled on JET, this scheme should be used for the development of the 20s high power discharges (45MW) foreseen after the completion of the NBI power enhancement that includes, not only an increase of the NBI power, but also of duration (from 10s to 20s).
- By changing the magnetic configuration, quasi-double null plasmas are able to reach a grassy ELM regime as defined by [54]. This approach has been successfully tested on JET where the

mild ELM regime has been combined, for the first time, with core ITB on the ion heat transport channel. In addition to the magnetic configuration requirement, this approach requires operation at high poloidal beta ($\beta_p \geq 1.6$). Therefore, grassy ELM regime at $q_{95} \sim 5$ has not been achieved due to the present lack of additional power. This technique requires a quasi-double-null configuration that might be difficult to sustain in JET at high power after the power upgrade (~45MW) due to the excessive power load on the upper part of the machine that was not designed to withstand such a high heat flux. Similarly, if it is confirmed that the plasma shape requirement is a necessary condition to obtain grassy ELMs, this regime could not extrapolate directly to ITER steady-state conditions (despite that the required $\beta_p 1$ could be reached). Nevertheless, part of the objective of this experiment is to investigate, ultimately, understand the conditions require for sustaining grassy ELMs, and finally, investigate how the domain of existence of grassy ELMs could be extended to ITER relevant conditions.

- By ergodising the toroidal magnetic field at the plasma edge. This approach has been successfully tested in the high triangularity/high $\beta_N$ scenario at reduced magnetic field. In this case, the reduction in confinement at the edge transport barrier was compensated by an increase of the core energy content. The mechanism of this enhancement needs to be further understood, but might be related to an increase of the shear of plasma toroidal rotation in the core due to a "magnetic braking" at the plasma edge. This approach should be considered, at this stage, to be a proof of principle, and has only been investigated in short duration pulses due to technical limitations of the EFCC system. However, this method of ELM mitigation deserves further study in future JET experiments.

Finally, an indication of the progress is illustrated in table 1 where the parameters of a high $\beta_N$ advanced scenario plasma developed on JET are compared to the ITER target parameters for steady-state operation. Despite the fact that progress has been made in terms of optimising the magnetic configuration, safety factor profile, increasing the plasma density and increasing $\beta_N$, a further major effort is required to increase the thermal energy content and the bootstrap current fraction on JET, in particular in wall-compatible scenarios. A possible route to further increase the core confinement at high density could be to increase the applied heating and current drive power. Indeed, operation at high (core and edge) density leads to a reduction of the:

(i) toroidal plasma rotation;
(ii) NBI penetration to the plasma core, and related core heating/fuelling;
(iii) efficiency of external non-inductive current drive systems;
(iv) electron temperature (since the power per particle goes down), leading to a faster current profile relaxation.

All these effects contribute to make the formation and sustainement of core ITBs more challenging when increasing the core and edge density. Therefore, higher heating and non-inductive current

[1] *The calculated $b_p$ for ITER steady-state reference scenario at 9MA is around 1.8 [52]*

drive power should be expected to compensate for the effects of increased density and allow the formation and sustainement of regimes with enhanced core confinement at high density. In this context, the future JET enhancements, which include a power upgrade together with the modification of the plasma facing components, will provide a unique opportunity to develop wall compatible scenarios at high fusion performance together with the high bootstrap current fraction required for steady-state.

**ACKNOWLEDGMENT**

The authors would like to acknowledge the JET-EFDA task-forces who did strongly contribute to the success of the experiments described in this paper, the Euratom-UKAEA Fusion Association as operator of the JET-facility for its dedicated support in particular in view of increasing the additional power in JET advanced scenarios, and our colleagues at the EFDA-JET close Support Units. We would like also to acknowledge fruitful discussions on the ITER requirements for steady state operation with our colleagues from the ITER international organisation in particular Drs V. Mukhovatov, A.S. Kukushkin and A.R. Polevoi.

**REFERENCES**

[1]. Albanese R. et al. 2005, Fusion Eng. Design, **74**, Issues 1-4 627

[2]. Andrew Ph et al 2007 Proc. of the 17th International Conf. on Plasma Surface Interactions, to appear in J. Nucl. Materials **363-365**

[3]. Ariola M. et al.2007, Plasma shape and boundary flux control at JET with XSC Proc. 34th EPS Conf. on Controlled Fusion and Plasma Physics (Varsaw, 2007)

[4]. Arnoux G. et al 2007 Plasma-wall heat loads in ITER-like advanced tokamak scenarios on JET Proc. 34th EPS Conf. on Controlled Fusion and Plasma Physics (Varsaw, 2007)

[5]. Beurskens M. et al 2007 Edge pedestal characterisation in high triangularity advanced tokamak scenarios with impurity seeding Proc. 34th EPS Conf. on Controlled Fusion and Plasma Physics (Varsaw, 2007)

[6]. Challis C.D. et al 1995 22nd EPS Conference on Plasma Phys. (Bournemouth, 1995) vol. 19C, II-069

[7]. Challis C.D. et al 2001 Plasma Phys. Control. Fusion **43** 861

[8]. Challis C.D. et al 2002 Plasma Phys. Control. Fusion **44** 1031

[9]. Challis C.D. et al 2007 High $\beta_N$ JET H-modes for steady-state application Proc. 34th EPS Conf. on Controlled Fusion and Plasma Physics (Varsaw, 2007)

[10]. Ciric D. et al 2006 Overview of the JET Neutral Beam Enhancement Project Proc. 24th Symp. On Fusion Technology, 11-15 Sep 2006 Warsaw, Poland, guest Ed. T. Wejrzanowski

[11]. Cesario R. et al 2007 Lower hybrid current drive in experiments for transport barriers at high $\beta_N$ of JET, Proceedings of the 17th Topical Conference on Radiofrequency power in plasmas, Clearwater, Florida, USA May 2007.

[12]. Colas L. et al 2007 submitted to Plasma Phys. Control. Fusion
[13]. Crisanti F. et al 2003 Plasma Phys. Control. Fusion **45** 379
[14]. Dumortier P. et al 2002, Plasma Phys. Control. Fusion **44** (2002) 1845
[15]. DurodiÈ F et al 2005 The ITER-like ICRF Antenna for JET Proc. 23rd Symp. On Fusion Technology, Ed. F. Gnesotto et al, Fusion Eng. Des. **74** 223 (special issue)
[16]. Dux Ret al 2004 Nucl. Fusion **44** 260
[17]. Federici G. et al 2003 J. Nucl. Mater **313-316** 11
[18]. Gauthier E, P. Andrew, G. Arnoux, Y. Corre and JET-EFDA contributors 2007 Journal of Nuclear Materials, **363-365**, 1026
[19]. Geraud A. et al 2006 The JET high frequency Pellet injector Project, Proc. 24th Symposium on Fusion Technology (Warsaw, 2006)
[20]. Gormezano et al 2007(a) Nucl. Fusion **47** S285 (ITER Physics Basis, Chapter 6)
[21]. Gormezano C. et al 2007(b) submitted to Fusion Science & Technology
[22]. Gormezano C. and the JET team 2001 Nucl. Fusion **41** 1327
[23]. Green B.J. et al 2003 Plasma Phys. Control. Fusion **45** 687
[24]. Gryaznevich M.P. et al 2007 Experimental identification of the beta limit in JET Proc. 34th EPS Conf. on Controlled Fusion and Plasma Physics (Varsaw, 2007)
[25]. Huber A et al Asymmetries in the JET Divertor Radiation Pattern during ELMs Proc. 34th EPS Conf. on Controlled Fusion and Plasma Physics (Varsaw, 2007)
[26]. ITER Physics Expert Groups on Confinement and Transport and Confinement Modelling and Database 1999, ITER Physics Basis (chapter 2) Nucl. Fus **39** 2175
[27]. Jachmich S. et al 2007 Langmuir probe measurements of particle and heat fluxes at the JET MkII-HD divertor targets Heat Proc. 34th EPS Conf. on Controlled Fusion and Plasma Physics (Varsaw, 2007)
[28]. Jackson et al 2002, Plasma Phys. Control. Fusion **44** 1893
[29]. Joffrin E. 2007(a) Advanced scenarios developments for the next step submitted to Plasma Phys. Control. Fusion
[30]. Joffrin E. et al. 2007(b) Stationary 20s Hybrid discharge in JET Proc. 5th IAEA Technical Meeting on Steady State Operations of Magnetic Fusion Devices, Daejeon, Rep. of Korea (2007)
[31]. Kamada Y. et al 2002 Plasma Phys. Control. Fusion **44** A279
[32]. Koslowski H R et al 2007 Type-I ELM mitigation in high triangularity and steady state regimes using low n external perturbation fields on JET Proc. 34th EPS Conf. on Controlled Fusion and Plasma Physics (Varsaw, 2007)
[33]. Kukushkin A.S. et al 2002 Nucl. Fusion **42**187
[34]. Kukushkin A.S. et al 2003 Fus. Eng. Design **65** 355
[35]. Kukushkin A.S. et al 2007 Nucl. Fusion **47** 698
[36]. Janeschitz G. et al 2002 Nucl. Fusion **42** 14

[37]. Lao L L, Ferron J R, Groebner R J, Howl W, St John H, Strait E J and Taylor T S 1990 Nucl. Fusion **30** 1035
[38]. Liang Y. et al 2007(a) Phys. Rev. Lett. **98** 265004
[39]. Liang Y. et al 2007(b) Active Control of Type-I Edge Localized Modes on JET Edge submitted to Plasma Phys. Control. Fusion
[40]. Lin-Liu Y.R. and Stambaugh R. 2004 Nucl. Fusion **44** 548
[41]. Litaudon X 2006 Plasma Phys. Control. Fusion **48** A1
[42]. Litaudon X et al 2007 Nucl. Fusion **47** 1285
[43]. Loarte et al 2007 Nucl. Fusion **47** S203 (ITER Physics Basis, Chapter 4)
[44]. Matthews G.F. et al 2007 Phys. Scr. T128 137
[45]. Moreau D. et al. 2006, New Dynamic-Model Approach for Simultaneous Control of Distributed Magnetic and Kinetic Parameters in the ITER-like JET Plasmas, Fusion Energy 2006 (Proc. 21st Int. Conf. Chengdu, 2006), IAEA-CN-149, IAEA, Vienna (2007), CD-ROM file ex_P1-2, http://www-naweb.iaea.org/napc/physics/FEC/FEC2006/html/node57.htm#14844.
[46]. Moreau D. et al. 2007, Real-Time Profile Control for Advanced Tokamak Operation on JET, Proc.5th IAEA Technical Meeting on Steady State Operations of Magnetic Fusion Devices, Daejeon, Rep. of Korea (2007).
[47]. Mailloux J. et al 2007 Development of ITB plasmas at high $\beta_N$ and high triangularity in JET Proc. 34th EPS Conf. on Controlled Fusion and Plasma Physics (Varsaw, 2007)
[48]. Pericoli et al 2007 Proc.5th IAEA Technical Meeting on Steady State Operations of Magnetic Fusion Devices, Daejeon, Rep. of Korea (2007).
[49]. Paméla J., Matthews G.F., Philipps V. and Kamendje R. 2007(a) J. Nucl Materials, **363-365** 1
[50]. Paméla J. et al 2007(b) The JET programme in support of ITER Proc. 24$^{th}$ Symp. On Fusion Technology, 11-15 Sep 2006 Warsaw, Poland, guest Ed. T. Wejrzanowski et al, to appear in Fusion Eng. Des. (special issue)
[51]. Pironti A. et al. 2007 A new algorithm for strike-point sweeping at JET Proc. 34th EPS Conf. on Controlled Fusion and Plasma Physics (Varsaw, 2007)
[52]. Polevoi A.R. et al 2007 Private Communication
[53]. Rimini F.G. et al 2005 Nucl. Fusion **45** 1481
[54]. Saibene G. et al 2005 Nuc. Fus. **45** 297
[55]. Sarazin Y. et al 2002 Plasma Phys. Control. Fusion **44** 2445
[56]. Tuccillo A.A.et al 2006 Nucl. Fusion **46** 214
[57]. Tresset G. et al 2002 Nucl. Fusion **42** 520
[58]. Villone F. et al 2007 Development of 20s long hybrid scenarios on JET Proc. 34th EPS Conf. on Controlled Fusion and Plasma Physics (Varsaw, 2007)
[59]. Weynants R.R. et al 1999 Nucl. Fusion **39** 1637

| | $q_{95}$ | $\kappa_x / \delta_x$ | $\beta_N$ | $n/n_{Gw}$ | $H_{IPB98(y,2)}$ | $I_{boot}/I_p$ |
|---|---|---|---|---|---|---|
| ITER steady-state target | 5 | 2/0.5 | 2.6-3 | 0.8-0.9 | 1.3-1.7 | 50% |
| **JET-AT (#70069) ($P_{rad}/P_{tot}$~20%)** | **5.2** | **1.8/0.45** | **2.8** | **0.6** | **1.1** | **30-40%** |

*Table 1*

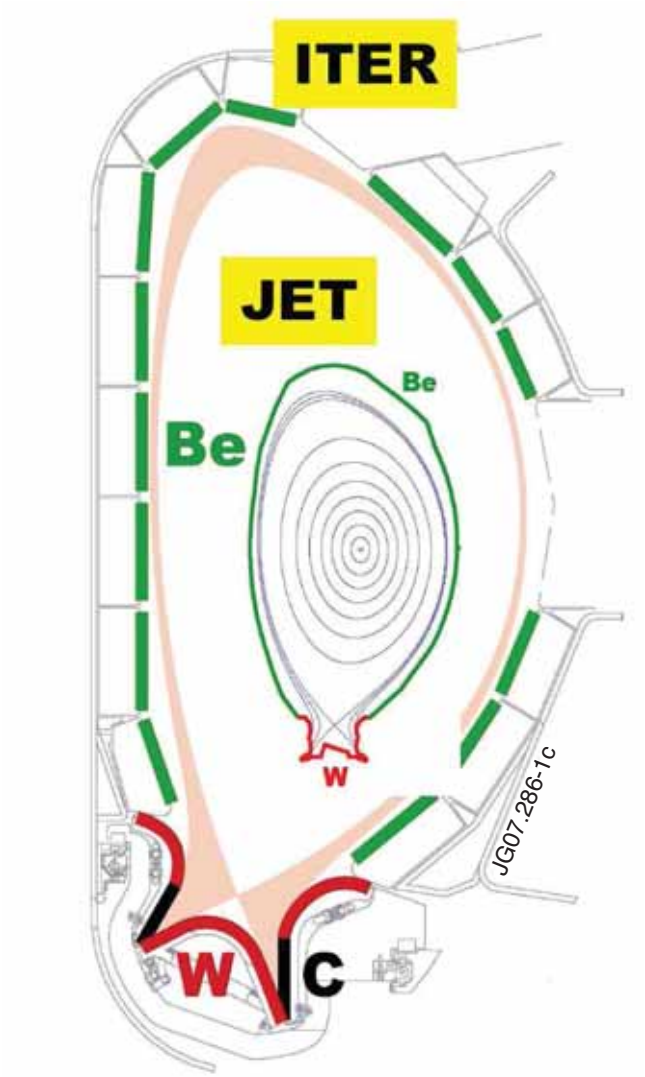


*Figure 1: Schematic diagram showing the poloidal cross-section of ITER and JET. The choice of plasma facing components is indicated for the present ITER design and for the JET-enhancement within the "ITER-like" wall project.*

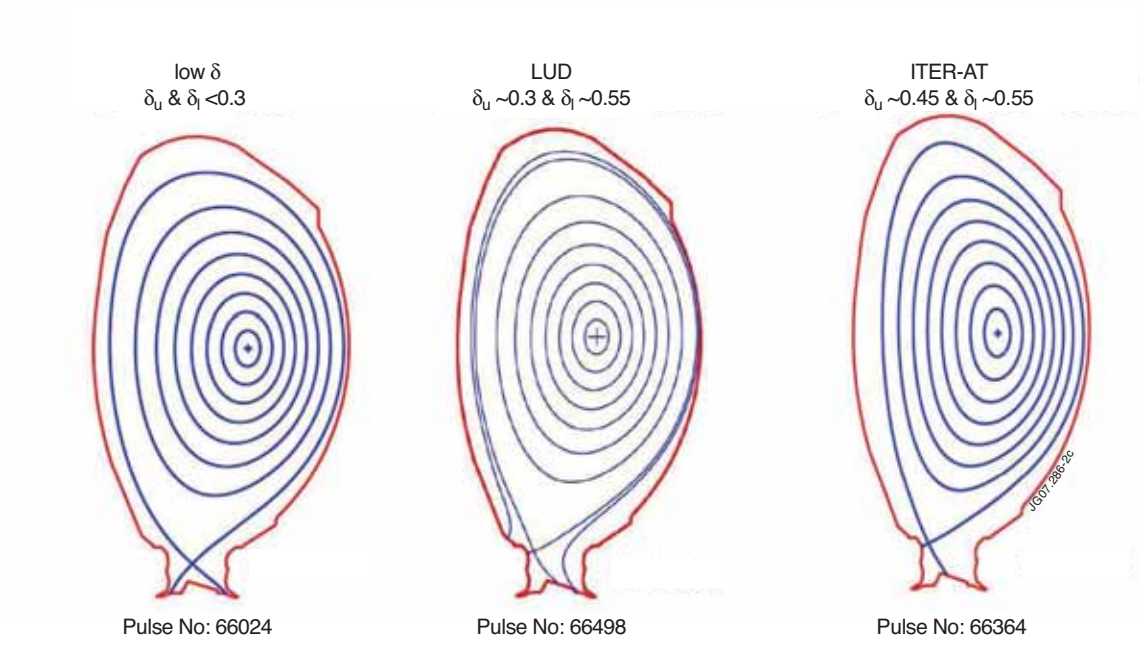


*Figure 2: Various magnetic configurations used in JET advanced scenarios. The magnetic field lines are computed with EFIT equilibrium reconstruction code (Lao et al 1990) constrained by the magnetic measurements. From left to right: low triangularity, LUD and ITER-AT magnetic configurations. LUD and ITER-AT were developed during the 2006-2007 experimental campaign.*

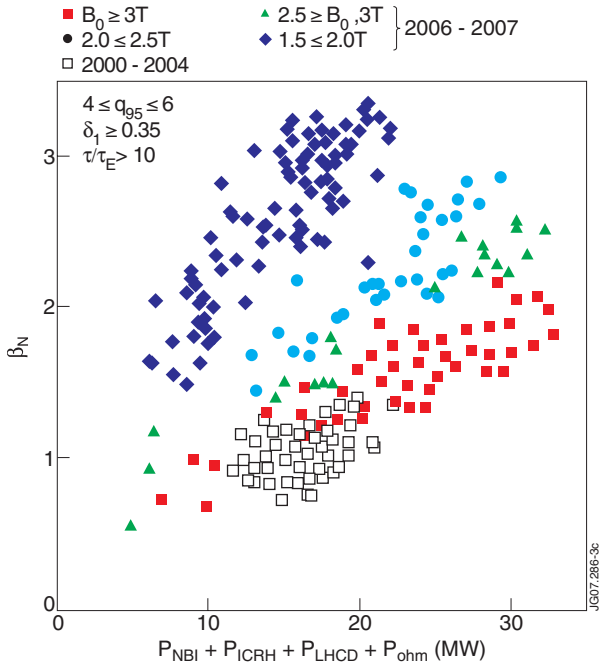


*Figure 3: $\beta_N$ plotted versus the total input power in the main heating phase for various toroidal magnetic field (each point corresponds to one discharge taken from the 2000-2007 JET-EFDA advanced scenario database). The data are selected at $4 \leq q_{95} \leq 6$, $\delta_l \geq 0.35$ (e.g. ITER-AT or LUD configuration), $\tau/\tau_E > 10$ where $\tau$ is the duration of high performance phase and $\tau_E$ the diamagnetic energy confinement time.*

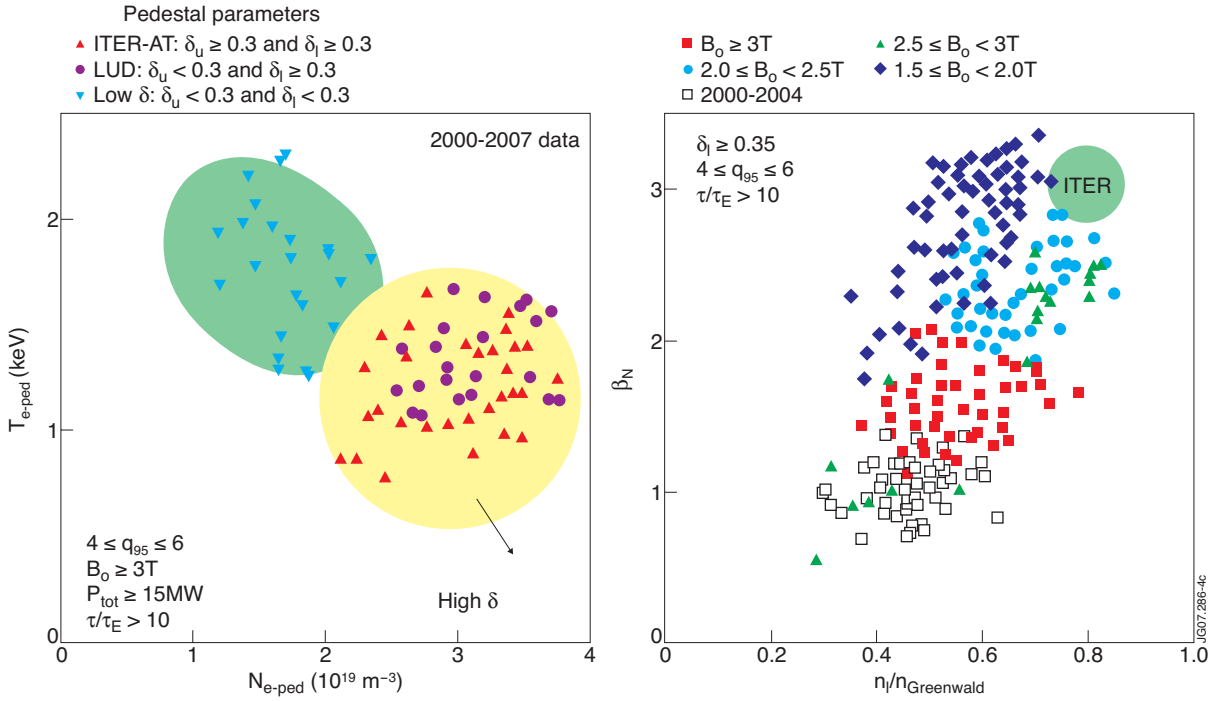


*Figure 4: (left) Electron temperature, $T_{e\text{-}ped}$, versus the electron density, $N_{e\text{-}ped}$, at the top of the edge transport barrier measured with the Thomson scattering diagnostic for the three typical configurations low triangularity, LUD and ITER-AT (see Fig. 2). The data are selected at $4 \leq q_{95} \leq 6$, $B_o \geq 3T$, $P_{tot} \geq 15MW$, $\tau/\tau_E > 10$. (right) $\beta_N$ plotted versus the line averaged density normalized to the Greenwald density, $n_l/n_{Gw}$ for various toroidal magnetic field. The data are selected at $4 \leq q_{95} \leq 6$, $\delta_l \geq 0.35$, $t/t_E > 10$ as in Fig. 3. Each point corresponds to one discharge taken from the 2000-2007 JET-EFDA advanced scenario database.*

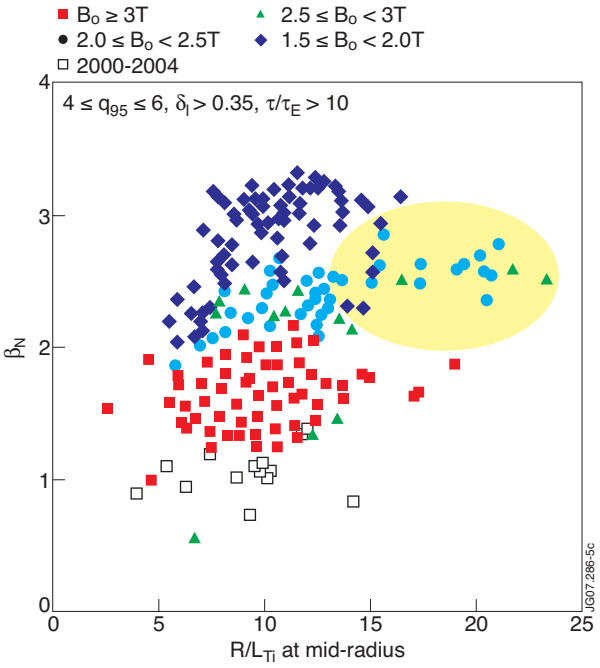


*Figure 5: $\beta_N$ versus£normalised ion temperature gradient $R/L_{Ti}$ estimated at mid-radius for various toroidal magnetic fields. The data are selected at $4 \leq q_{95} \leq 6$, $\delta_l \geq 0.35$, $t/t_E > 10$ as in Fig. 3. Each point corresponds to one discharge taken from the 2000-2007 JET-EFDA advanced scenario database.*

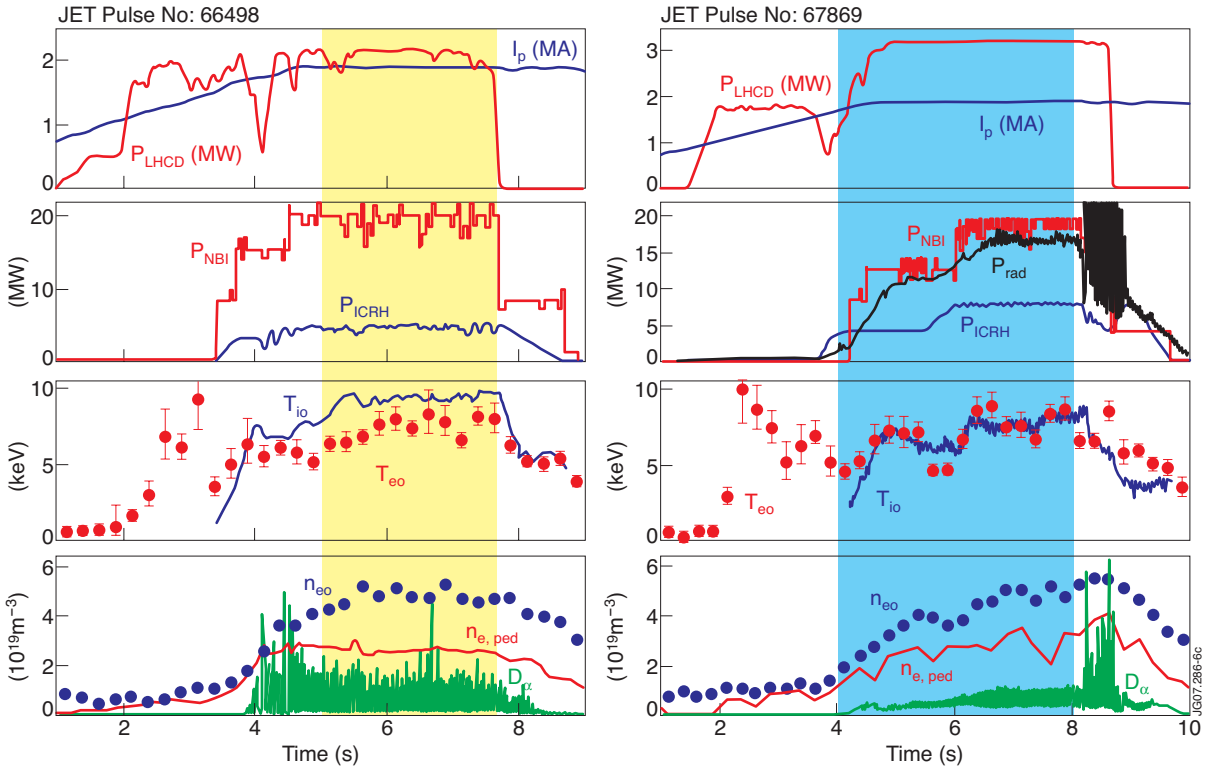


*Figure 6: Time evolution of the main parameters of two high power discharges in LUD magnetic configuration with $B_o$~3.1T/$I_P$~1.9MA, $q_{95}$~5 but with two different values of $P_{rad}/P_{tot}$. (left) JET Pulse No: 66498 without neon injection during the high power phase, $P_{rad}/P_{tot}$~30% (right) JET discharge No: 67869 with neon injection between 4s and 8s, $P_{rad}/P_{tot}$~55%. (Ip, plasma current; $P_{LHCD}$, LHCD power; $P_{NBI}$, NBI power; $P_{ICRH}$, ICRH power, $T_{io}$, core ion temperature from charge exchange recombination spectroscopy; $T_{eo}$ core electron temperature from Thomson Scattering; $n_{eo}$ core electron temperature from Thomson Scattering; $N_{e\text{-}ped}$ pedestal electron density; $D_\alpha$ from visible spectroscopy).*

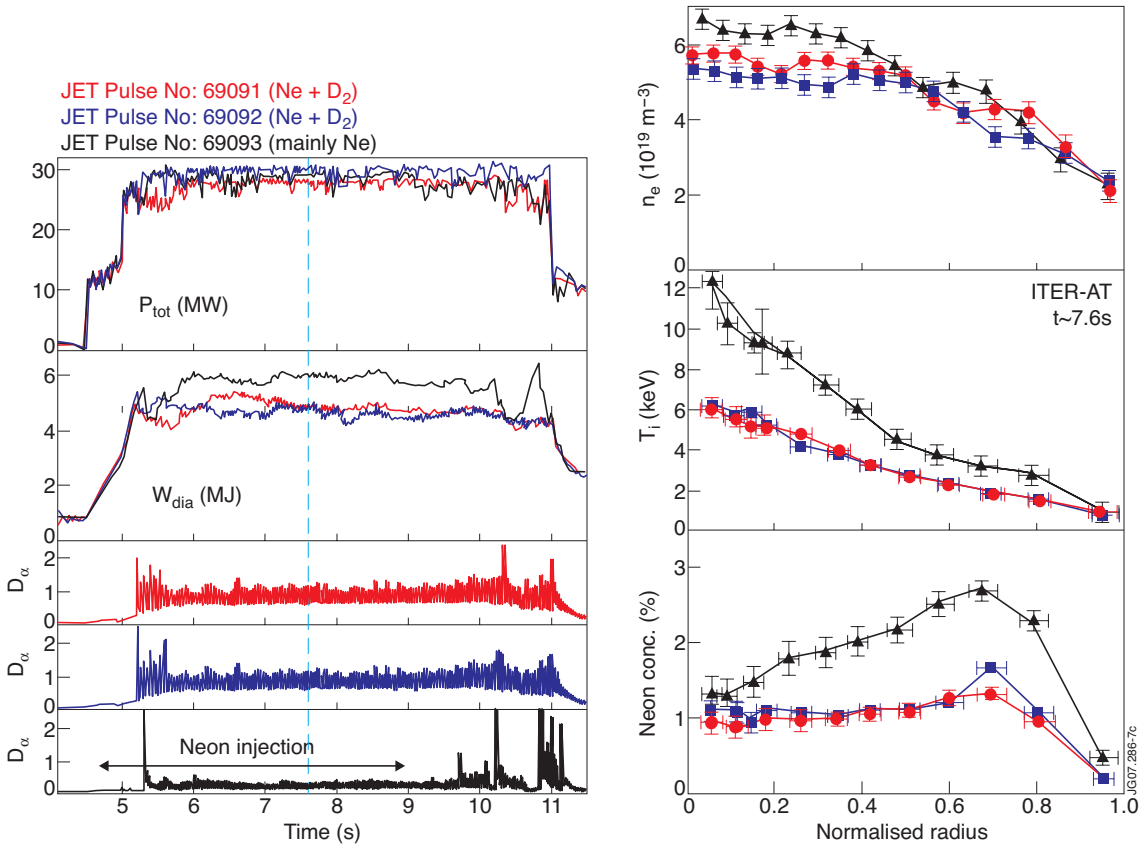


*Figure 7:(left) Time evolution of high power/high triangularity (ITER-AT magnetic configuration, $B_o$~3.1T/$I_P$~1.9MA) discharges: total applied power, diamagnetic energy content and $D_\alpha$ time traces for the JET Pulse No's: 69091 (red), 69092 (blue), 69093 (black); (right) profiles of electron density, $n_e$, $T_i$ and neon concentration versus the normalised toroidal flux at t~7.6s (c.f. arrow on the time traces) for the same discharges.*

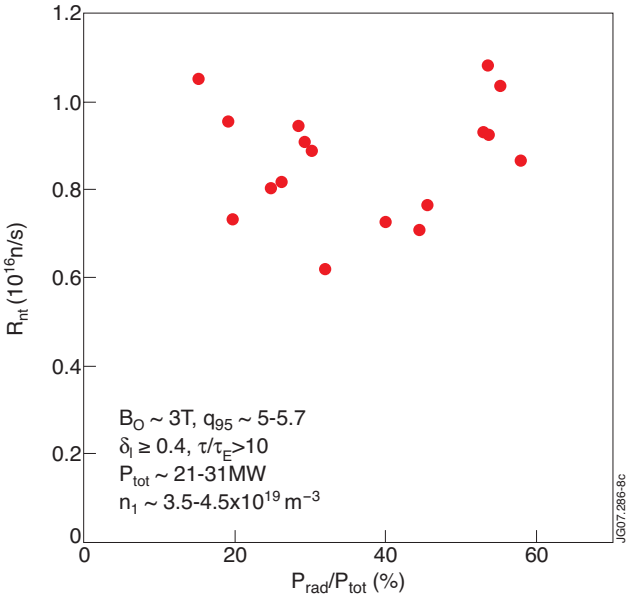


*Figure 8: Neutron yield, $R_{nt}$, (beam-target dominated) versus the radiated power fraction for high triangularity discharges (inter-ELMs values for the radiated power). Data selected at $B_o$~3T, 5 ≤ $q_{95}$ ≤ 5.7, $P_{tot}$~21-31MW, $n_l$~3.5-4.5×$10^{19}$$m^{-3}$, $\delta_l$ ≥ 0.4, $\tau/\tau_E$>10. Each point corresponds to a discharge taken in the 2006-2007 JET advanced tokamak database.*

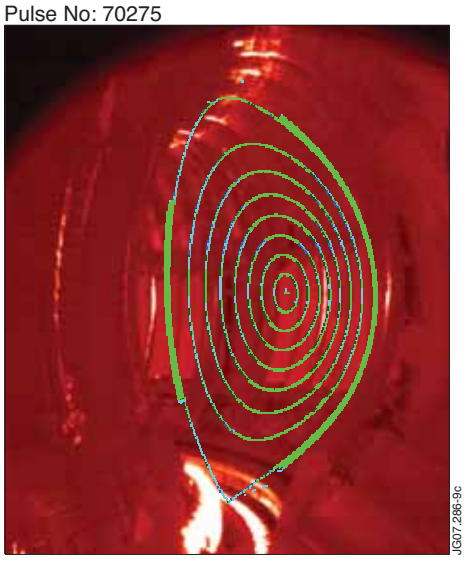


*Figure 9: Infra-Red image of the JET in-vessel PFC measured with the new wide angle camera. High triangularity ($B_o$~3.1T/$I_P$~1.9MA, ITER-AT magnetic configuration) JET Pulse No: 70275 at t~9.5s: a total power of 24MW is applied during 6s (144MJ).*

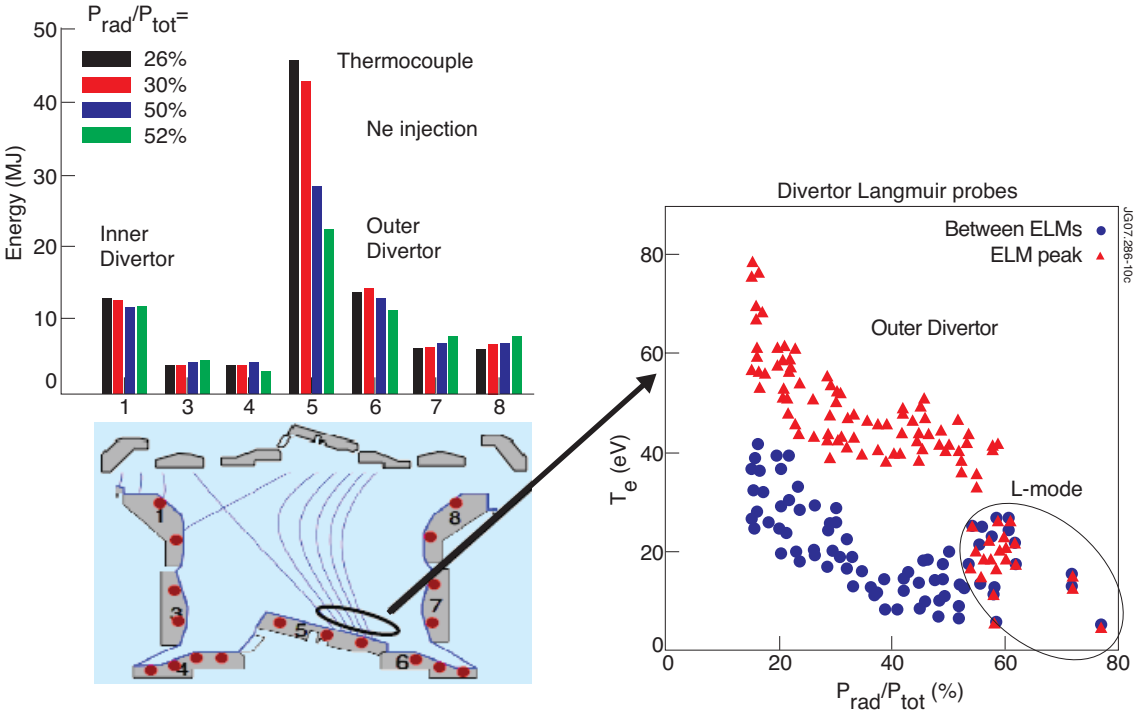


*Figure 10 (left) Energy distribution in the divertor versus the tile number measured by the thermocouples embedded in the tiles (schematically represented by the red dots in divertor cross-section) for various levels of radiated fraction $P_{rad}/P_{tot}$ [%] (JET Pulse No's: 69987, 69981, 70291, 70285); (right) Electron temperature measured by the divertor Langmuir probes located on the LBSRP close to the outer strike point versus $P_{rad}/P_{tot}$. The blue and red points correspond respectively to the measurement between ELMs and at the ELM peak. The radiated powers are measured with the vertical bolometer camera and the values between ELMs are systematically used.*

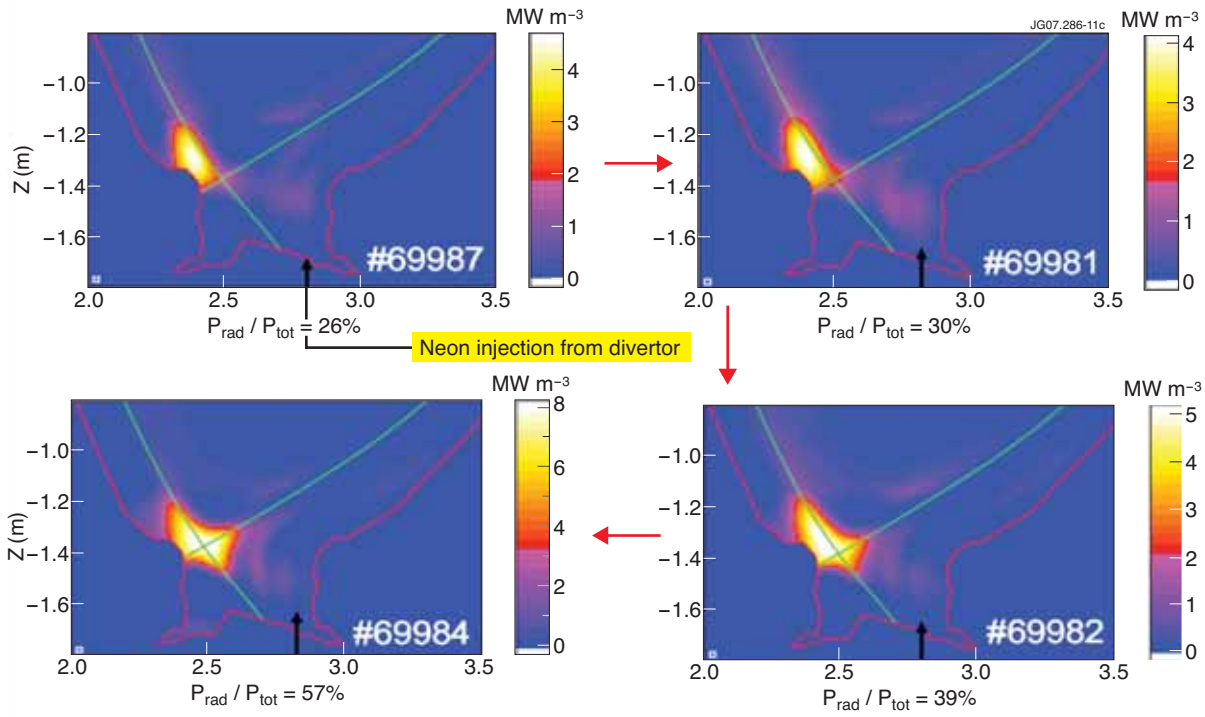


*Figure 11: Divertor radiation pattern as deduced from the newly installed bolometer camera for four discharges (JET Pulse No's: 69987, 69981, 69984, 69982, $B_o$~3.1T/$I_P$~1.9MA, ITER-AT magnetic configuration) with different levels of $P_{rad}/P_{tot}$ (inter-ELMs values for the radiated power). Neon is injected from a ring of gas injection modules located in the base plate of the outer divertor.*

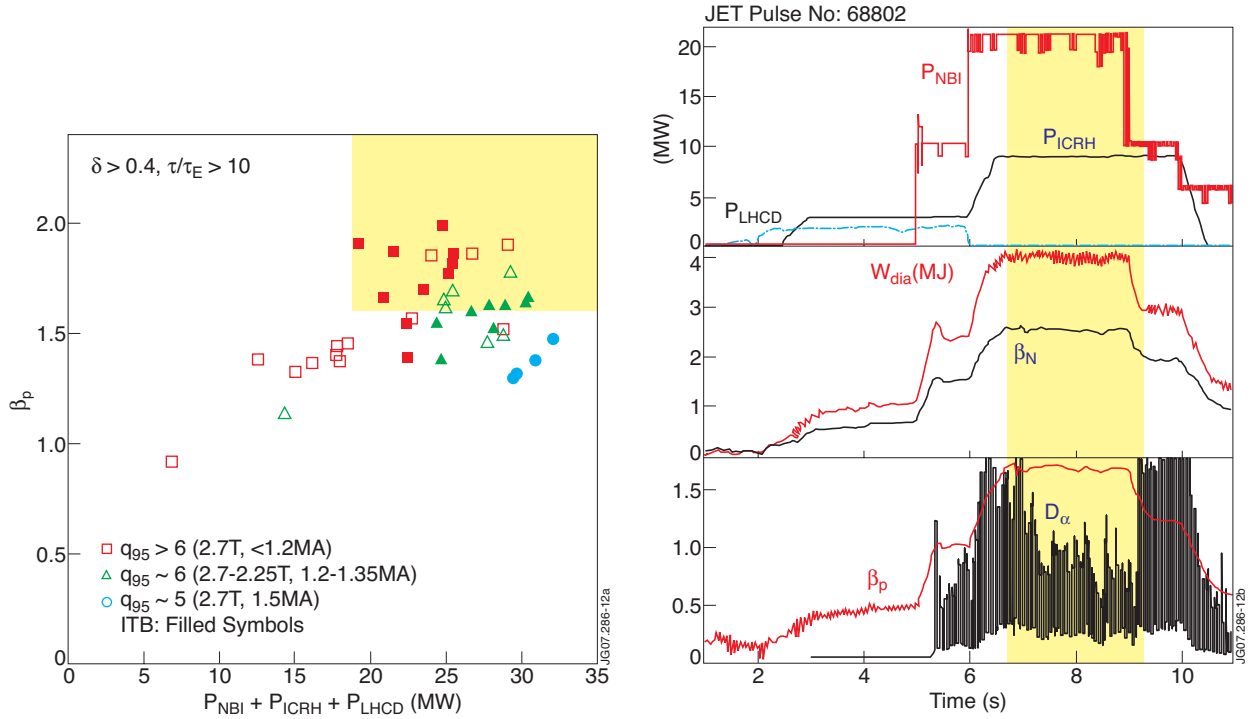


*Figure 12: (left) Poloidal beta, $\beta_{p,}$ versus the total applied power in the main heating phase for various $q_{95}$ values in a Quasi-double Null magnetic configuration (each point corresponds to one discharge taken from the 2000-2007 JET-EFDA advanced scenario database). The symbols are filled when an ITB on the ion temperature profile is detected; (right) Time evolution of the main parameters of a high-$\beta_p$ Quasi-double Null discharge with grassy-ELMs. JET Pulse No: 68802, $I_p$~1.35MA, $B_o$~2.7T and $q_{95}$~6, $\delta$~0.5, $n_l$~$4.1\times10^{19}m^{-3}$, $n_l/n_{Greenwald}$~0.8.*

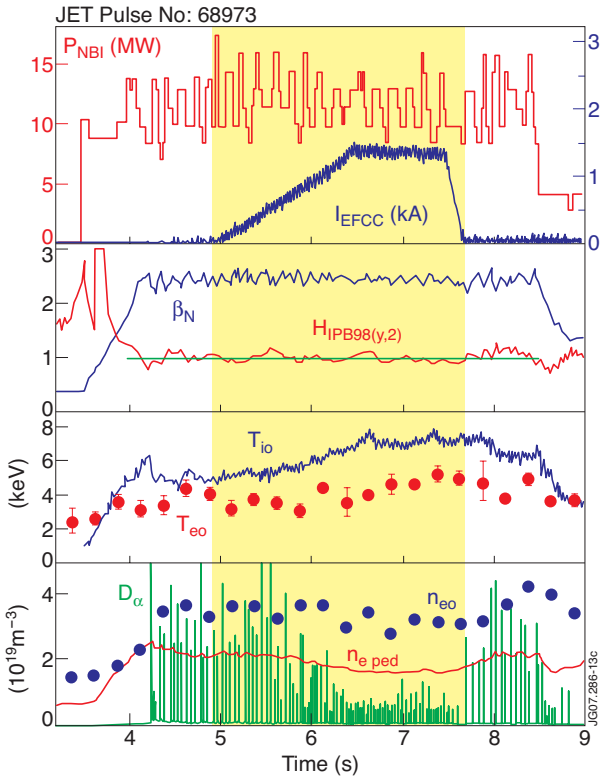


*Figure 13: Time evolution of the main parameters of a high-$\beta_N$ / high triangularity discharge where EFCC perturbation (n=1 mode) is applied to mitigate the Type I-ELM activity. JET Pulse No: 68973, Ip~1.3MA, $B_o$~1.8T and $q_{95}$~4.5.*